Journal of Medical Ultrasonics (2020) 47:535–548
https://doi.org/10.1007/s10396-020-01059-x

SPECIAL FEATURE: REVIEW ARTICLE

Diagnosis and assessment of nonalcoholic fatty liver disease / nonalcoholic steatohepatitis using ultrasound elastography

Magnetic resonance imaging for the assessment of pathological hepatic findings in nonalcoholic fatty liver disease

Kento Imajo[1] · Yasushi Honda[1] · Masato Yoneda[1] · Satoru Saito[1] · Atsushi Nakajima[1]

Received: 18 August 2020 / Accepted: 25 September 2020 / Published online: 27 October 2020

Abstract
The prevalence of nonalcoholic fatty liver disease (NAFLD) is expected to increase because of the current epidemics of obesity and diabetes, and NAFLD has become a major cause of chronic liver disease worldwide. Liver fibrosis is associated with poor long-term outcomes in patients with NAFLD. Additionally, increased mortality and liver-related complications are primarily seen in patients with nonalcoholic steatohepatitis (NASH); however, nonalcoholic fatty liver (NAFL) is believed to be benign and non-progressive. Therefore, distinguishing between NASH and NAFL is clinically important. Liver biopsy is the gold standard method for the staging of liver fibrosis and distinguishing between NASH and NAFL. Unfortunately, liver biopsy is an invasive and expensive procedure. Therefore, noninvasive methods, to replace biopsy, are urgently needed for the staging of liver fibrosis and diagnosing NASH. In this review, we discuss the recent studies on magnetic resonance imaging (MRI), including magnetic resonance elastography, proton density fat fraction measurement, and multiparametric MRI (mpMRI) that can be used in the assessment of NASH components such as liver fibrosis, steatosis, and liver injury including inflammation and ballooning.

Keywords Magnetic resonance elastography · Proton density fat fraction · Corrected-T1 · Nonalcoholic fatty liver disease · Nonalcoholic steatohepatitis

Introduction

Nonalcoholic fatty liver disease (NAFLD) has become a major cause of chronic liver disease worldwide. Its prevalence is currently estimated to be 25% in the general population [1, 2], 90% in those with obesity, and 60% in those with type 2 diabetes mellitus [3–5]. The prevalence of NAFLD is expected to increase because of the current epidemics of obesity and diabetes [6]. Additionally, liver fibrosis has been reported to be strongly associated with the long-term outcomes in patients with NAFLD [7, 8].

Liver biopsy is the recommended gold standard method in the diagnosis of nonalcoholic steatohepatitis (NASH) and staging of liver fibrosis in patients with NAFLD [9]. However, because of high costs, possible risks, and requirement for healthcare resources, an invasive liver biopsy is a poorly suited diagnostic test for such a prevalent condition [10]. Therefore, alternatives to liver biopsy, including biochemical tests and assessments of liver stiffness measurement (LSM), are being developed [11]. LSM is a promising surrogate biomarker of the stage of liver fibrosis, and several elastography techniques are currently available for the same, including magnetic resonance elastography (MRE) [12, 13]. In this review, we discuss the recent studies on the use of magnetic resonance imaging (MRI), including MRE, in the assessment of liver fibrosis and other pathological findings, such as steatosis, inflammation, and ballooning in NAFLD.

✉ Atsushi Nakajima
nakajima-tky@umin.ac.jp

[1] Department of Gastroenterology and Hepatology, Yokohama City University Graduate School of Medicine, Yokohama 236-0004, Japan

Magnetic resonance elastography for the assessment of liver fibrosis in NAFLD

MRE was developed at the Mayo Clinic in 1995 [14], introduced into clinical practice in 2007, and approved by the FDA in 2010. It is an MRI-based technique for

quantitative imaging of tissue stiffness and is currently the most accurate noninvasive imaging method available for diagnosing liver fibrosis [15–18]. MRE is currently available on MR scanners of three major manufacturers (General Electric, Milwaukee, WI, USA; Philips Medical Systems, Best, Netherlands; Siemens Healthineers, Erlangen, Germany) with 1.5-T and 3-T field strengths.

If there is a dedicated device and software for the generation and analysis of liver elastic wave propagation, quantitative stiffness images (elastograms) of the liver can be rapidly obtained during breath-holding and can, therefore, be readily included in the conventional liver MRI protocols [19]. The volume of the liver that is measurable using MRE is typically ≥ 250 mL and up to a third of the liver volume [20, 21]. A more advanced version of three-dimensional (3D) MRE, which is commercially not available at present, can evaluate the entire liver volume and was used in a recent prospective study [22]. Therefore, MRE can be used to assess the entire liver with a high success rate [23]. Furthermore, unlike ultrasonography (US)-based techniques, the success of MRE is operator-independent [18] and is minimally affected by obesity [15]. MRE is also highly repeatable; the inter-observer and intra-observer reproducibility among the scanners is high [24–27]. The failure rate of MRE was estimated to be approximately 1% in an unscreened population [28] and 5% in patients with various liver diseases [29], with substantial iron deposition in the liver being the most common cause of failure. The technical failure rate associated with iron deposition is higher with 3 T MR systems than with 1.5 T MR systems because of the stronger susceptibility effect of iron. Patients who are claustrophobic and have MR-incompatible implants cannot tolerate MR exams. Additionally, motion artifacts such as cardiac impulses are also a cause of failure because MRE is a motion-sensitive technique. MRE should be conducted after ≥ 4 h of fasting because LSM may increase due to postprandial portal blood flow [30].

An increasing number of studies have demonstrated that MRE is an accurate method for diagnosing and staging hepatic fibrosis in NAFLD (Table 1). Among the studies that used MRE, the AUROC for the diagnosis of stage > 1, > 2, > 3, and 4 was 0.772–0.869, 0.856–0.919, 0.870–0.981, and 0.882–0.993, respectively [31–38]. In the most recent meta-analysis by Xiao et al., which included 5 studies and 628 patients with NAFLD, the AUROCs for the diagnosis of stages 2, 3, and 4 fibrosis using MRE were 0.88, 0.93, and 0.92, respectively [39]. In a systematic review, the authors concluded that MRE might have the highest diagnostic accuracy for the staging of liver fibrosis (Fig. 1) [38]. The optimal MRE thresholds were 2.61, 2.97, 3.62, and 4.69 kPa, respectively, for the detection of any (stage ≥ 1), significant (stage ≥ 2), and advanced (stage ≥ 3) fibrosis and cirrhosis (stage ≥ 4) in patients with NAFLD [38].

MRE has several advantages over US-based elastography in the evaluation of liver fibrosis. Xiao et al. [39] conducted a systematic review and meta-analysis, which included 64 articles and 13,046 patients with NAFLD, to compare the diagnostic performances of noninvasive indices (aspartate aminotransferase-to-platelet ratio index (APRI], fibrosis-4 index (FIB-4], BARD score, NAFLD fibrosis score (NFS], vibration-controlled transient elastography (VCTE) [M and XL probe], shear wave elastography (SWE), and MRE in the prediction of significant fibrosis, advanced fibrosis, and cirrhosis; they found that MRE offered the best diagnostic performance for the staging of liver fibrosis. Other studies have also demonstrated that MRE is superior to VCTE and noninvasive indices in the diagnosis of liver fibrosis in patients with NAFLD [22, 34–36]. Since MRE has the highest accuracy in the diagnosis of liver fibrosis, it is increasingly regarded as a promising surrogate for the monitoring of disease progression and assessment of therapeutic endpoints [40]. The most recent prospective cohort study by Ajmera et al. [41] investigated the clinical utility of MRE in predicting the progression of fibrosis in patients with NAFLD with paired biopsies and paired MRE measurements. The authors reported that a 15% increase in MRE was associated with histologic progression of fibrosis. More recently, Honda et al. suggested in their review article, which summarized the meta-analysis of MRE, that MRE had good diagnostic accuracy over US-based elastography techniques in the assessment of liver fibrosis [42].

Proton density fat fraction (PDFF) measurement to assess steatosis in NAFLD

PDFF is the ratio of MRI-visible protons bound to fat to all protons in the liver (bound to fat and water); it is an MRI-based method for quantitatively assessing hepatic steatosis and is available from several manufacturers of MRI scanners. Chemical shift imaging is applied to separate the liver signal into water and fat components by acquiring the gradient echoes at appropriately spaced echo times. In some variants of this approach, only the magnitude data are retained while the phase data are discarded. These variants accurately quantify hepatic PDFF from 0 to 50%, which fortuitously captures the biological range of human hepatic steatosis, which rarely exceeds 50% [43]. Scan protocol parameters, such as flip angle and echo times, the fat signal model, and T2*-corrections are sensitive variables influencing the PDFF measurement [44]. Grimm et al. indicated that multi-point Dixon sequences, but not two-point sequences, should be used for PDFF measurements [44]. The precision and reproducibility of MRI-PDFF measurement have been explored. Negrete

Table 1 Magnetic resonance elastography in patients with NAFLD

Design	Strength of static magnetic field (Tesra)	Comparison with scoring system	Comparison with US elastography	Fibrosis stage	Cutoff value (kPa)	AUROC	Se	Sp	PPV	NPV	Reference
Retrospective	1.5 T	Yes	No	Stage ≥ 3	4.15	0.954	0.85	0.93	ND	ND	Kim et al
Single center											Radiology. 2013; 268(2): 411–419.(30)
N = 142											
Cross-sectional Prospective	3.0 T	No	No	Stage ≥ 1	3.02	0.838	0.554	0.907	0.911	0.542	Loomba et al. Hepatology. 2014; 60(6): 1920–1928. (31)
Single center				Stage ≥ 2	3.58	0.856	0.657	0.915	0.767	0.862	
N = 117				Stage ≥ 3	3.64	0.924	0.864	0.905	0.679	0.966	
				Stage 4	4.67	0.894	0.8	0.944	0.571	0.981	
Individual participant data pooled analysis. *N* = 232	1.5 or 3.0 T	No	No	Stage ≥ 1	2.88	0.86	0.75	0.77	ND	ND	Singh et al
				Stage ≥ 2	3.54	0.87	0.79	0.81	ND	ND	Eur Radiol. 2016; 26(5): 1431–40.(32)
				Stage ≥ 3	3.77	0.9	0.83	0.86	ND	ND	
				Stage 4	4.09	0.91	0.88	0.87	ND	ND	
Cross-sectional Prospective	3.0 T	Yes	Yes	Stage ≥ 1	2.5	0.8	0.75	0.857	0.99	0.846	Imajo et al
Single center			Vs. VCTE (M probe)	Stage ≥ 2	3.4	0.89	0.873	0.85	0.884	0.836	Gastroenterology. 2016;150(3): 626–637. (33)
N = 142				Stage ≥ 3	4.8	0.89	0.745	0.869	0.745	0.81	
				Stage 4	6.7	0.97	0.909	0.945	0.588	0.992	
Cross-sectional	3.0 T	No	Yes	Stage ≥ 1	2.99	0.799	0.583	0.906	0.894	0.615	Cui et al. Hepatology. 2016; 63(2): 453–61.(34)
Single center			Vs. ARFI	Stage ≥ 2	3.62	0.885	0.667	0.957	0.846	0.889	
N = 125				Stage ≥ 3	3.62	0.934	0.905	0.933	0.731	0.98	
				Stage 4	4.15	0.882	0.889	0.914	0.444	0.991	
Cross-sectional Prospective	3.0 T	No	No	Stage ≥ 1 (3D,40 Hz)	1.77	0.848	ND	ND	ND	ND	Loomba et al. Am J Gastroenterol. 2016; 111(7): 986–94. (22)
Single center	2D (60 Hz) and 3D-MRE (40 or 60 Hz)			Stage ≥ 2(3D,40 Hz)	2.38	0.856	ND	ND	ND	ND	
N = 100				Stage ≥ 3(3D,40 Hz)	2.43	0.981	1	0.937	0.722	1	
				Stage 4 (3D,40 Hz)	3.21	0.993	ND	ND	ND	ND	

Table 1 (continued)

Design	Strength of static magnetic field (Tesra)	Comparison with scoring system	Comparison with US elastography	Fibrosis stage	Cutoff value (kPa)	AUROC	Se	Sp	PPV	NPV	Reference
Cross-sectional Prospective	3.0 T	No	Yes	Stage ≥ 1	2.65	0.82	0.765	0.791	0.813	0.739	Park et al. Gastroenterology. 2017; 152(3): 598–607. (35)
Single center			Vs. VCTE (M and XL probe)	Stage ≥ 2	2.86	0.89	0.793	0.818	0.657	0.898	
$N = 104$				Stage ≥ 3	2.99	0.87	0.778	0.803	0.483	0.938	
				Stage 4	3.35	0.87	0.75	0.814	0.273	0.972	
Cross-sectional Prospective	3.0 T	No	No	Stage ≥ 1	2.78	0.772	0.444	0.907	0.762	0.71	Schwimmer et al. Hepatology. 2017; 66(5): 1474–1485. (36)
Multi-center											
$N = 90$. Child				Stage ≥ 3	3.33	0.894	0.333	0.905	0.2	0.95	
Retrospective pooled data analysis. Multi-center. $N = 230$	1.5 or 3.0 T	No	Yes	Stage ≥ 1	2.61	0.869	0.713	0.726	0.849	0.541	Hsu et al. Clin Gastroenterol Hepatol. 2019; 17(4): 630–637 (37)
				Stage ≥ 2	2.97	0.919	0.849	0.854	0.798	0.893	
				Stage ≥ 3	3.62	0.93	0.825	0.832	0.618	0.935	
				Stage 4	4.69	0.942	0.8	0.859	0.408	0.972	

et al. [45] demonstrated high inter-examiner agreement in participants with obesity for each hepatic segment (intraclass correlation (ICC) ≥ 0.992, standard deviation (SD) ≤ 0.66%, range ≤ 1.24%), lobe (ICC ≥ 0.998, SD ≤ 0.34%, range ≤ 0.64%), and whole liver (ICC = 0.999, SD ≤ 0.24%, range ≤ 0.45%). Similar intra- and inter-examiner precisions were demonstrated in overweight and obese participants by Tyagi et al. [46]. Bannas et al. [47] further demonstrated significantly smaller variance with excellent intra- and inter-observer agreement and repeatability with MRI-PDFF compared with histologic grading of steatosis ($P < 0.001$). Vu et al. [48] suggested that MRI-PDFF quantification methods should sample each liver segment in both lobes and include a total surface area ≥ 5 cm^2 to provide accurate estimate of the mean liver PDFF.

MRI-PDFF correlates with the histologically determined grade of steatosis in patients with NAFLD. Studies that used MRI-PDFF measurement reported that AUROCs for the diagnosis of grade > 1, grade > 2, and stage 3 were 0.960–0.990, 0.825–0.90, and 0.79–0.92, respectively. The corresponding MRI-PDFF cutoffs for mild steatosis (grade > 1) ranged from 3.5 to 8.9%, with a sensitivity of 89%–97% and specificity of 88%–100% (Table 2) [34, 36, 49–51]. Imajo et al. [34] directly compared and demonstrated that MRI–PDFF measurement had higher accuracy than VCTE-based controlled attenuation parameter (CAP) in diagnosing steatosis in patients with NAFLD. However, they only assessed VCTE using the M probe. More recently, using a well-characterized, prospective cohort of American adults with biopsy-proven NAFLD, Park et al. [36] compared the accuracy of VCTE-based CAP measurement using both M and XL probes and compared it with that of MRI-PDFF measurement in diagnosing steatosis in patients with NAFLD; they demonstrated that MRI-PDFF measurement was superior to CAP measurement using M and XL probes. More recently, Runge et al. [52] demonstrated that MR spectroscopy-derived PDFF measurement was superior to CAP measurement in detecting and grading liver steatosis in human NAFLD.

Multiparametric MRI (mpMRI)

The utility of MRE has been demonstrated for identifying patients with NASH from those with simple steatosis [52] and from those with advanced fibrosis in chronic liver disease [53]. However, it has not exhibited sufficient utility for longitudinal monitoring of fibrosis [54, 55]. Furthermore, there is conflicting evidence regarding the effects of body mass index (BMI) on the MRE failure rates and its diagnostic performance [29, 56, 57].

Multiparametric MRI (mpMRI) measurements of hepatic steatosis (PDFF) and iron-corrected T1 (cT1) are emerging as promising quantitative imaging biomarkers

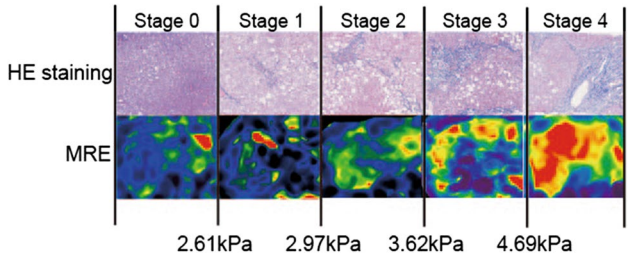

Fig. 1 Pathological fibrosis and MRE images with optimal threshold values from representative patients with stage 0, 1, 2, 3, and 4 fibrosis, respectively

for NASH. MpMRI is now standardized across all major MRI platforms and is available in several countries. MRI-PDFF has excellent correlation with histologically graded steatosis across the clinical range seen in NAFLD [58] and high diagnostic accuracy in stratifying all grades of liver steatosis [59–61], and cT1 has been demonstrated to correlate with ballooning [62]. More importantly, it has been demonstrated to predict the clinical outcomes in patients with chronic liver disease [63]. Additionally, the AUROCs in mpMRI were 0.69, 0.74, and 0.80, respectively, while differentiating between NASH and NAFL and while considering cT1 as an index test in the differentiation between NAS < 5 and ≥ 5 for the same index test, and in the diagnosis of NASH using liver inflammation and fibrosis (LIF) score [62, 63]. An optimal cutoff for LIF has recently been identified with a sensitivity of 91% and specificity of 52%. For cT1, as well, an optimal cutoff (875 ms) has been suggested to distinguish between low- and high-risk (NASH or fibrosis > 1) patients with sensitivity and specificity of 97% and 50%, respectively. Both metrics have demonstrated excellent technical validity with high repeatability and reproducibility across MRI manufacturers and field strengths [64]. The technical validation and precision afforded by mpMRI techniques, as well as their sensitivity to subtle changes in hepatic fat and fibro-inflammation, have resulted in their increasing inclusion as endpoints in NASH clinical trials, as well as inclusion in the FDA and EMA Biomarker Qualification Programs.

The diagnosis of NASH is currently based on the histological presence of steatosis, lobular inflammation, and ballooning. The presence of fibrosis, in addition to these pathological findings, suggests more advanced disease. It is important to note, however, that the only biomarkers demonstrated to predict the outcomes in these patients are histological fibrosis and MRI cT1 [65]. Of these, cT1 is sensitive to steatosis, ballooning, and inflammation, as well as fibrosis, and, therefore, cannot be a pure biomarker of fibrosis. An actual measurement image and details on the above report

Table 2 Proton density fat fraction in patients with NAFLD

Design	Comparison with controlled attenuation parameter	Steatosis grade	Cutoff value (%)	AUROC	Se	Sp	PPV	NPV	Reference
Cross-sectional prospective single center *N* = 51	No	Grade ≥ 1	8.9	ND	ND	ND	ND	ND	Permutt et al. Aliment Pharmacol Ther. 2012; 36(1): 22–29. (47)
		Grade ≥ 2	16.3	ND	ND	ND	ND	ND	
		Grade 3	25.02	ND	ND	ND	ND	ND	
Cross-sectional prospective single center *N* = 77	No	Grade ≥ 1	6.4	0.989	0.97	1.00	1.00	0.71	Tang et al. Radiology. 2014; 267(2): 422–31.(48)
		Grade ≥ 2	17.4	0.825	0.61	0.90	0.90	0.61	
		Grade 3	22.1	0.893	0.68	0.91	0.72	0.90	
Cross-sectional prospective single center *N* = 142	Yes Vs. VCTE (M probe)	Grade ≥ 1	5.2	0.96	0.900	0.933	0.892	0.519	Imajo et al Gastroenterology. 2016;150(3): 626–637.(33)
		Grade ≥ 2	11.3	0.90	0.789	0.841	0.845	0.784	
		Grade 3	17.1	0.79	0.737	0.810	0.632	0.953	
Cross-sectional prospective single center *N* = 27. Child	No	Grade ≥ 1	3.5	ND	0.890	0.880	ND	ND	Di Martino M et al. World J Gastroenterol. 2016; 22(39): 8812–8819.(49)
		Grade ≥ 2	ND	ND	ND	ND	ND	ND	
		Grade 3	ND	ND	ND	ND	ND	ND	
Cross-sectional prospective single center *N* = 104	Yes Vs. VCTE (M and XL probe)	Grade ≥ 1	3.71	0.99	0.958	1.000	1.000	0.700	Park et al. Gastroenterology. 2017; 152(3): 598–607. (35)
		Grade ≥ 2	13.03	0.90	0.800	0.833	0.750	0.870	
		Grade 3	16.37	0.92	0.818	0.836	0.450	0.966	
Prospective single center *N* = 55	Yes Vs. VCTE (M probe)	Grade ≥ 1	4.14	0.99	0.940	1.000	1.000	0.625	Rung JH et al. Radiology. 2018 Feb;286(2):547–556. (50)
		Grade ≥ 2	15.72	0.98	0.923	0.966	0.960	0.933	
		Grade 3	20.88	0.96	1.000	0.826	0.529	1.000	

on mpMRI in the assessment of the pathogenesis of NAFLD are presented in Fig. 2 and Table 3.

MRI technologies for the assessment of steatohepatitis in NAFLD

MRE was evaluated for diagnosing NASH in six studies; the AUROCs ranged from 0.70 to 0.79 with sensitivity and specificity of 72% and 87%, respectively, for NAS ≥ 5 in studies that did not include fibrosis in the NASH definition, and similar results were observed in a subset of patients without fibrosis [22, 34, 36, 53, 54]. Among MR non-elastographic techniques (Table 3), the ^{31}PMRS-derived ratio between nucleotide triphosphates (α-peak) and triphosphates (αNTP/TP), which reflects cellular energy failure [66], and the concentration of specific metabolites (e.g., alanine, lactate, and triglycerides), which are assessed using ^{1}H-MRS [67], were used to diagnose the severity of NAFLD. It demonstrated AUROCs of 0.71 for αNTP/TP and 1.00 for alanine, with the latter being evaluated in a small sample of 26 patients with NAS ≥ 5.

Other MRI approaches include quantitative susceptibility imaging, intravoxel incoherent motion (IVIM) diffusion-weighted MRI, and morphological evaluations, such as liver volume and preperitoneal fat area, all evaluated in a single study, with AUROCs of 0.61, 0.68, and 0.74 for different IVIM parameters and 0.91 for susceptibility; the last one was tested in a small sample of 32 patients [68–71]. Furthermore, a score based on MRI optical analysis estimators produced an AUROC of 0.83 with sensitivity and specificity of 87% and 60%, respectively [72]. In the case of contrast media-based approaches, gadoxetic acid enhancement in the hepatobiliary phase exhibited sensitivity and specificity of 97% and 63% in a retrospective study in 81 patients, whereas superparamagnetic iron oxide (SPIO) and ultrasmall SPIO (USPIO)-enhanced MRI-derived ΔR2* yielded sensitivity and specificity of up to 91% and 73%, respectively, for USPIO in a study in 25 patients with NAS ≥ 5 [73–75]. Nowadays, USPIO is not commercially available all over the world, and SPIO is available only in Japan. The direct consequences of the test on the health, qualitative analysis of resource consumption, operator-dependence, and state-of-the-art level of the techniques are summarized in Table 3.

Multifrequency magnetic resonance elastography

Diagnostic threshold levels for staging fibrosis vary as a result of varying technical setups and vibration frequencies in MRE. Previous studies in volunteers and a limited number of patients have demonstrated that the complex shear modulus of liver, G*, depends on the dynamic test range by demonstrating a clear frequency dispersion [76, 77]. The real part, G', of the complex modulus is determined by the

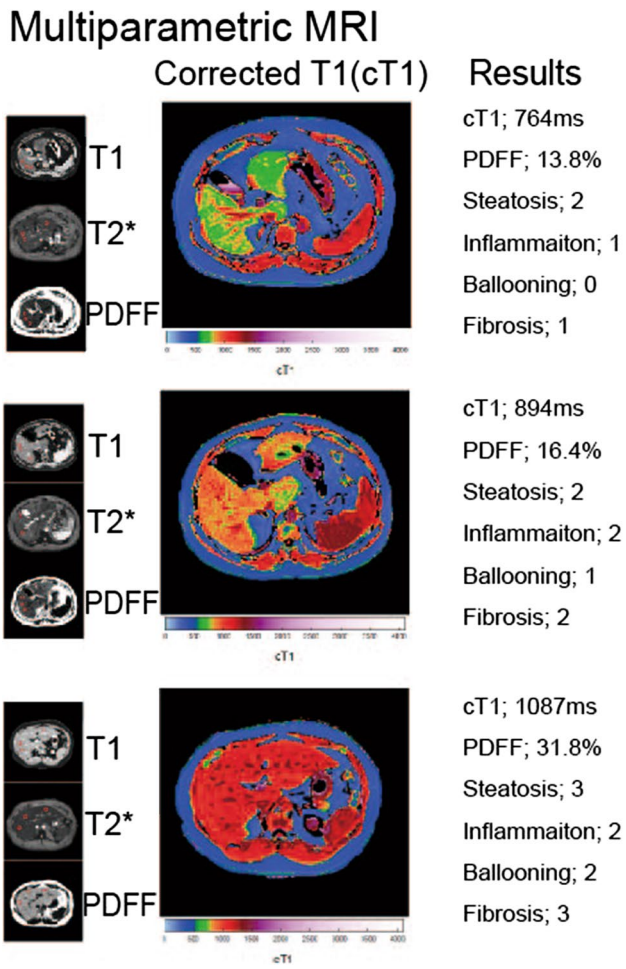

Fig. 2 Examples of multiparametric MRI (mpMRI) in patients with NAFLD. Representative images from patients in each severity category (NAS = 3 + Fibrosis = 1, NAS = 5 + Fibrosis = 2, NAS = 7 + Fibrosis = 3), produced by analysis of the raw data using mpMRI

restoration of the mechanical energy owing to the elastic properties of the material, whereas the imaginary part, G'', of the complex modulus is associated with viscous properties due to the inherent mechanical friction of the tissue [78]. Both parameters are independent and important measures of the mechanical constitution of materials and tissues. Viscoelasticity models the dispersion of G' and G'', which results in generalized material parameters sensitive to the mechanical connectivity and integrity of tissue on a microstructural level. To date, elasticity-based staging of hepatic fibrosis has been performed using vibration data that are accumulated at a single frequency and, therefore, our current knowledge about the frequency-dependent viscoelastic properties of the different stages of liver fibrosis is limited. Multifrequency MRE (MMRE) has recently been demonstrated to be sensitive in the early detection of subtle alterations in the viscoelasticity of the brain due to physiological

Table 3 Non-elastographic techniques in patients with NAFLD

Techniques	Design	Diagnostic ability (AUROC)	Cutoff value	Se	Sp	PPV	NPV	Reference
Multiparametric MRI (Liver MultiScan)- corrected T1 (cT1)	Prospective single center $N=71$ (NASH; $N=46$)	0.80 for NASH based on LIF score	1.4 based on LIF score	91.0	52.0	ND	ND	Pavlides et al. Liver Int. 2017;37:1065-1073. (62)
	Prospective single center $N=50$ (NASH; $N=38$)	0.69 for NASH based on cT1	875 ms based on cT1	97.5	50.0	88.6	83.3	Eddowes et al. Aliment Pharmacol Ther . 2018 Mar;47(5):631–644. (63)
31P-MRS	Cross-sectional prospective single center $N=151$ (NASH; $N=95$)	0.71 for NASH based on a-NTP/TP	16.36% based on a-NTP/TP	91.0	16.0	65.0	50.0	Abrigo et al. J Hepatol. 2014;60:809-815. (64)
1H-MRS	Cross-sectional prospective single center $N=26$ (NASH; $N=11$)	1.00 for NAS ≥ 5 based on Alanine (Ala)	16.04% based on Ala	100.0	100.0	ND	ND	Kim et al J Magn Reson Imaging. 2017;46:1298-1310. (65)
		0.78 for NAS ≥ 5 based on lactate + trygliceride (Lac + TG)	360.8% based on Lac + TG	82.0	67.0	ND	ND	
Diffusion weighted (DW) MRI	Cross-sectional prospective single center $N=59$ (NASH; $N=22$)	0.742 for NASH based on pure molecular-based (D)	0.760 s/mm2 based on D	69.3	65.6	ND	ND	Parente et al. PLoS ONE. 2015;10(5):e0125653 (67)
		0.678 for NASH based on perfusion-related (D*)	41.45 s/mm2 based on D*	68.5	71.4	ND	ND	
		0.607 for NASH based of vascular fraction (f)	34.23 s/mm2 based on f	48.5	69.7	ND	ND	
Imaging biomarkers for MRI	Cross-sectional prospective single center $N=126$ (NASH; $N=65$)	0.88 for NASH in estimation cohort based on NASHMRI score (N = 39)	0.5 based on NASHMRI score	87.0	74.0	80.0	82.0	Gallego et al. Sci Rep. 2016;6:31,421.(70)
		0.83 for NASH in validation cohort based on NASHMRI score ($N=87$)	0.5 based on NASHMRI score	87.0	60.0	71.0	81.0	
Quantitative susceptibility MRI	Retrospective single center $N=81$ (NASH; $N=35$)	0.91 for NASH based on magnetic susceptibility	ND	ND	ND	ND	ND	Leporq et al. NMR Biomed. 2017; 30(10). https://doi.org/10.1002/nbm.3766 (66)
Gadoxetic acid–enhanced magnetic resonance (MR) imaging	Retrospective single center $N=32$ (NASH; $N=20$)	0.85 for NASH based on gadoxetic acid relative enhancement	1.24 based on gadoxetic acid relative enhancement	97.0	63.0	ND	ND	Bastati et al. Radiology. 2014;271(3):739-747. (71)
SPIO/USPIO-enhanced MRI	SPIO prospective single center $N=19$ (NASH; $N=10$)	0.79 for NAS ≥ 5 based on relative decrease in T2 (%T2)	32.5 based on %T2	73.0	88.0	70.0	89.0	Tomita et al. J Magn Reson Imaging. 2008;28:1444-1450. (73)
		0.83 for NAS ≥ 5 based on relative decrease in time constant (T)	42.8 s based on T	67.0	100.0	77.0	100.0	
	USPIO prospective single center $N=24$ (NASH; $N=13$)	0.87 for NAS ≥ 5 based on ΔR2*	45.5 s-1 based on ΔR2*	77.0	91.0	ND	ND	Smits et al. Radiology. 2016;278(3):782-791. (72)
MRI Liver Volume	Retrospective single center $N=69$ (NASH; $N=37$)	0.741 for NAS ≥ 5 based on liver volume	ND	ND	ND	ND	ND	Dillman et al. AJR. 2018;210:166-174

Table 3 (continued)

Techniques	Design	Diagnostic ability (AUROC)	Cutoff value	Se	Sp	PPV	NPV	Reference
MRI visceral fat area and peritoneal fat area	Prospective single center $N=66$ (NASH; $N=23$)	ND	5cm2 based on preperitoneal fat area	93.0	55.0	ND	ND	Parente et al. J Gastroenterol Hepatol. 2018;33:511-517
			109cm2 based on visceral fat area	77.0	79.0	ND	ND	

aging and multiple sclerosis [79, 80]. Therefore, MMRE is a promising technique for staging liver fibrosis and distinguishing normal liver from that in the early stages of fibrosis. Several investigations have demonstrated that liver stiffness can have a static component that is primarily determined by extracellular matrix composites and structure (e.g., hepatic fibrosis) and a dynamic component that is affected by intrahepatic hemodynamic changes (e.g., inflammation, ballooning, congestion, and portal hypertension) [77–80]. The ability to distinguish how these components contribute to tissue stiffness and how the contributions change over the course of different diseases will have important diagnostic and prognostic implications and will direct translational research in NAFLD. However, the value of mechanical properties, other than shear stiffness, in distinguishing the different pathophysiologic states of the liver is yet to be established in NAFLD.

MRE in the assessment of portal hypertension in chronic liver disease including NAFLD

Liver fibrosis is the most important risk factor of portal hypertension in chronic liver diseases, including NAFLD. At the Baveno IV Consensus Workshop in Europe, clinically significant portal hypertension (CSPH) was defined using LSM obtained using VCTE [81]. MRE can noninvasively estimate LSM as well as VCTE, and LSM has been reported to correlate significantly with wedge hepatic venous pressure (WHVP), hepatic venous pressure gradient (HVPG), and portal hypertension in patients with chronic liver diseases, including NAFLD [82]. In a Korean study of 126 patients with chronic liver diseases, including NAFLD, an AUROC of 0.859 was observed to have good diagnostic performance in the diagnosis of esophageal varices (EVs) when the cutoff value of LSM of MRE was set at 4.63 kPa [83]. In our previous report, in 276 patients with chronic liver diseases, including NAFLD, a cutoff value of 4.2 kPa for LSM of MRE in the diagnosis of EV resulted in an AUROC of 0.850 and a cutoff value of 4.8 kPa for LSM of MRE for the diagnosis of EV for treatment indication (high-risk EV), and the AUROC had good diagnostic performance of 0.840 for EV. Additionally, comparing the criteria using VCTE (Baveno IV criteria) proposed at the Baveno IV Consensus workshop with the modified Baveno IV criteria using MRE, we found that the diagnosis of the presence of EV and the diagnosis of high-risk varices was better in MRE based criteria than VCTE-based criteria. We reported that the modified Baveno IV criteria have a high diagnostic ability [84]. These results suggest that LSM of MRE is useful in predicting portal hypertension in chronic liver diseases, including NAFLD.

It is known that portal hypertension is associated with splenomegaly; however, recently it has been reported that spleen stiffness measurement (SSM) is elevated in these

patients. Although the details of the pathogenesis remain unclear, it has been suggested that spleen congestion and spleen fibrosis may be involved in the pathogenesis of EV; a study of VCTE reported that SSM was more useful in the diagnosis of EV than LSM [85]. However, measurement of SSM using VCTE has several drawbacks. One is that VCTE is difficult to measure in the absence of splenomegaly. Another disadvantage is that the measurement limit of VCTE is 75 kPa; therefore, if SSM exceeds 75 kPa, it is difficult to measure it using VCTE [86]. Although VCTE for measuring SSM is currently being developed, it is difficult to use in Japan. However, MRE can measure LSM and evaluate SSM if the vibration reaches the spleen simultaneously (Fig. 3). It has been reported that SSM correlates more strongly with HVPG than with LSM, and that it can aid in diagnosing CSPH with high accuracy [87]. Shin et al. [88] suggested that SSM should be above the cutoff of 7.6 kPa and reported higher diagnostic ability of EVs than measurement of spleen length and volume. The authors also evaluated the usefulness of SSM in diagnosing EV in 511 patients with chronic liver diseases, including NAFLD (Fig. 3); they reported an AUROC of 0.92 at a cutoff of 9.4 kPa and 0.91 at a cutoff of 10.3 kPa in the diagnosis of high-risk EV (unpublished data, American Association for the Study of Liver Disease (AASLD) 2018.). Table 4 summarizes previous reports on portal hypertension and MRE in patients with chronic liver diseases, including NAFLD. SSM may be more useful in the diagnosis of portal hypertension than LSM. The use of criteria based on LSM (modified Baveno IV criteria in combination with platelets) or SSM for MRE, such as the diagnosis of CSPH exclusion using VCTE and platelets as advocated at the Baveno VI Consensus Workshop, can prevent unnecessary endoscopies in chronic liver diseases, including NAFLD. This would provide significant benefits, such as reduced medical costs and avoidance of complications.

Benefits and limitations of MRI in the assessment of NAFLD

A comparison between US elastography and MRI including MRE is presented in Table 5. One of the benefits of MRI is that it allows a much larger sampling compared with US techniques and liver biopsy, which may reduce the sampling variability secondary to the heterogeneity of fibrosis. Additionally, it has been proven that MRE generally provides more reliable measurements and fewer failures in patients with obesity or ascites. In a recent retrospective review of a large series of 1377 cases of MRE from the Mayo Clinic, the reported failure rate was less than 6%, with no effects of BMI on the failure rate [89]. MRI may also be a better candidate than US elastography in assessing the response to new therapies for NASH.

The limitations of MRE include the possibility of failure in patients with iron overload (using gradient echo sequence), cost and availability, and possible contraindications in patients with devices such as metallic splinters, vascular clips, and cochlear implants (Table 5). Additionally, LSM obtained using MRE may be influenced by extrahepatic cholestasis and acute liver injury [90, 91]. However, all major vendors now propose MRE capabilities, and new sequences such as echoplanar imaging have been demonstrated to decrease the failure rate in the presence of hepatic iron deposition. Although the US or MRI technique has advantages and limitations, VCTE and MRE are believed to be the methods of choice. According to the clinical practice

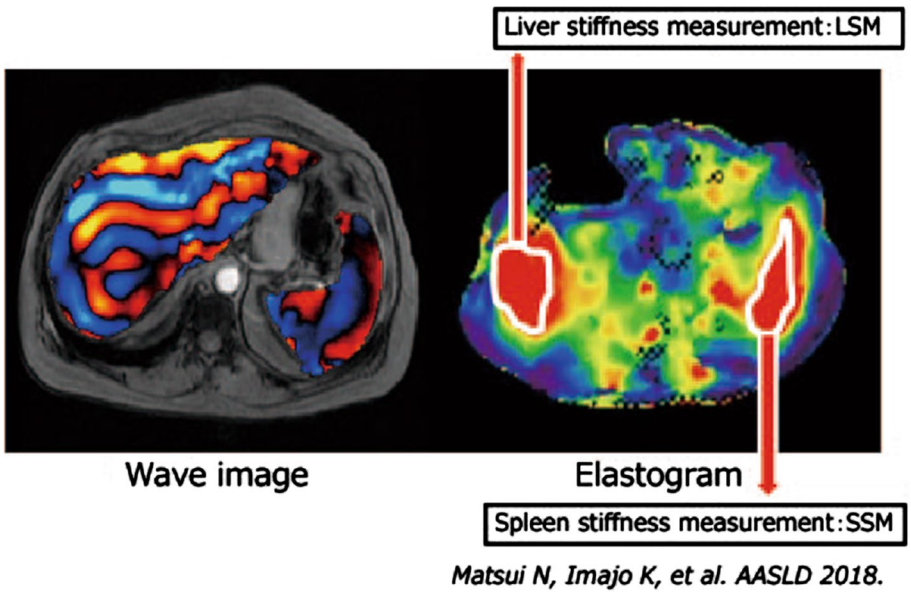

Fig. 3 Measurements of liver stiffness and spleen stiffness for the assessment of portal hypertension (left: wave image, right: elastogram)

Table 4 The assessment of portal hypertension using MRI in patients with chronic liver disease including NAFLD

Design	Country	Cutoff values and diagnostic ability for any EV (AUROC)	Cutoff values and diagnostic ability for high-risk EV (AUROC)	References
Retrospective, single center, $n=139$, MRE	Korea	LSM:4.58 kPa (0.821) SSM:7.23 kPa (0.833)	LSM:4.81 kPa (0.755) SSM:7.60 kPa (0.750)	Shin SU et al. Radiology 2014; 272: 143–153. (86)
Retrospective, single center, $n=126$, MRE	Korea	LSM:4.63 kPa (0.859) SSM:ND	LSM:5.80 kPa (0.810) SSM:ND	Sun HY et al. J Magn Reson Imaging 2014; 39: 559–566. (81)
Prospective, single center, $n=36$, MMRE	France	ND	Gl for spleeen:84 Hz:4.2 kPa (0.930)	Ronot M et al. Eur Radiol 2014; 24: 1394–1402. (80)
Retrospective, multi-center, $n=627$, MRE + Plts	Japan	LSM:4.20 kPa (0.850) SSM:ND	LSM:ND SSM:ND	Matsui N, et al. Gastroenterol Hepatol 2018; 33: 2022–2028.(82)
Retrospective, single center, $n=84$	Korea	LSM:ND SSM:ND	GRE-MRE LSM:4.493 kPa (0.752) SE-EPI-MRE LSM:5.880 kPa (0.839)	Kim YS et al. Eur Radiol 2017; 27: 4120–4128

AUROC area under the receiver operating characteristic, *EV* esophageal varices, *LSM* liver stiffness measurement, *MRE* magnetic resonance elastography, *Plts* platelets, *SSM* spleen stiffness measurement

guidelines published by the European Association for the Study of the Liver (EASL), VCTE is an acceptable noninvasive procedure for the identification of patients at low risk of advanced fibrosis or cirrhosis [92]. Additionally, according to the practice guidelines published by AASLD, VCTE and MRE are clinically useful tools in the identification of advanced fibrosis in patients with NAFLD [11]. However, other US elastographies are not recommended in the current guidelines for NAFLD. One of the reasons is that there are no follow-up data using other US elastographies in patients with NAFLD. Additionally, VCTE also has the advantage that it can be used to evaluate liver fibrosis and liver steatosis

Table 5 Comparison between US elastography and MR elastography

	US elastography	MR elastography
Sampling volume of liver	Little	Much*
HCC screening	Possible (except TE)	Possible with other sequence
Convenience of use	Good *	Poor
Inter-operator reproducibility	Good ICC; TE 0.98, ARFI 0.81, SWE 0.88	Good ICC; 0.99
Intra-operator reproducibility	Good ICC; TE 0.98, ARFI 0.81, SWE 0.88	Good ICC;
Evaluation of liver fat accumulation	Available using only TE-based CAP But the diagnostic accuracy is insufficient	Available using PDFF Good *
Ascites	Available if ascites is a little (except TE)	Available if ascites is a little Good *
Obesity	Possible for ARFI, SWE, TE by XL probe	Good *
Measurements of iron deposition	Not available	Available *
Effect of Iron overload on liver stiffness and liver fat accumulation	No effect *	Effect
Contraindications	No *	Biocompatible metal Pregnancy
Cost	Low *	High
Available institutions	Many *	Few

* Benefit

using a controlled attenuation parameter (CAP), which can measure the degree of ultrasound attenuation [93]. Recently, the FibroScan-AST (FAST) score combined with measurement of liver stiffness and CAP measured using VCTE and aspartate aminotransferase (AST) was proposed [94]. This score can identify patients with NASH (NAFLD activity score ≥ 4 and fibrosis stage ≥ 2) and has been validated in large global cohorts, even in Japan [95]. Furthermore, MRI-PDFF measurement is an MRI-based method for quantitatively assessing hepatic steatosis and is available as an option in MRI scanners from several manufacturers [49, 96].

Conclusions

MRI, including MRE, provides higher diagnostic performance in noninvasive detection of not only liver fibrosis, but also steatosis, inflammation, and ballooning in patients with NAFLD compared with other noninvasive methods. However, MRI techniques are relatively recent and have not been widely validated in NAFLD. Additionally, there are few reports on the usefulness of other technologies, including mpMRI and MMRE, in diagnosing NAFLD. Therefore, there is no consensus regarding the use of these elastography techniques in clinical practice in place of liver biopsy. Nevertheless, MRI appears to be best suited for the evaluation of pathological findings of the liver in patients with NAFLD. Several clinical algorithms for the diagnosis and monitoring of patients with NAFLD using MRE have been proposed [53, 97, 98]. Further research will validate these observations in patients with NAFLD.

Compliance with ethical standards

Conflict of interest Kento Imajo, Yasushi Honda, Masato Yoneda, Satoru Saito, and Atsushi Nakajima declare that they have no conflicts of interest.

Ethical statements All procedures followed were in accordance with the ethical standards of the responsible committee on human experimentation (institutional and national) and with the Helsinki Declaration of 1964 and later versions.

Informed consent Informed consent was obtained from all patients for being included in the study.

References

1. Younossi ZM, Keonig AB, Abdelatif D, et al. Global epidemiology of nonalcoholic fatty liver disease-Meta-analytic assessment of prevalence, incidence, and outcomes. Hepatology. 2016;64:73–84.
2. Li J, Zou B, Yeo YH, et al. Prevalence, incidence, and outcome of non-alcoholic fatty liver disease in Asia, 1999–2019: a systematic review and meta-analysis. Lancet Gastroenterol Hepatol. 2019;4:389–98.
3. Machado MP, Marques-Vidal P, Cortez-Pinto H. Hepatic histology in obese patients undergoing bariatric surgery. J Hepatol. 2006;45:600–6.
4. Milic S, Lulic D, Stimac D. Non-alcoholic fatty liver disease and obesity: biochemical, metabolic and clinical presentations. World J Gastroenterol. 2014;20:9330–7.
5. Dai W, Ye L, Wen SW, et al. Prevalence of nonalcoholic fatty liver disease in patients with type 2 diabetes mellitus: a meta-analysis. Med (Baltim). 2017;96:e8179.
6. Estes C, Anstee QM, Arias-Loste MT, et al. Modeling NAFLD disease burden in China, France, Germany, Italy, Japan, Spain, United Kingdom, and United States for the period 2016–2030. J Hepatol. 2018;69:896–904.
7. Angulo P, Kleiner DE, Dam-Larsen S, et al. Liver fibrosis, but no other histologic features, is associated with long-term outcomes of patients with nonalcoholic fatty liver disease. Gastroenterology. 2015;149:e10.
8. Hagström H, Nasr P, Ekstedt M, et al. Fibrosis stage but not NASH predicts mortality and time to development of severe liver disease in biopsy-proven NAFLD. J Hepatol. 2017;67:1265–73.
9. Cadranel JF. Good clinical practice guidelines for fine needle aspiration biopsy of the liver: past, present and future. Gastroenterol Clin Biol. 2002;26:823–4.
10. Ratziu V, Charlotte F, Heurtier A, et al. Sampling variability of liver biopsy in nonalcoholic fatty liver disease. Gastroenterology. 2005;128:1898–906.
11. Chalasani N, Younossi Z, Lavine JE, et al. The diagnosis and management of nonalcoholic fatty liver disease: practice guidance from the American association for the study of liver diseases. Hepatology. 2018;67:328–57.
12. Yoneda M, Imajo K, Takahashi H, et al. Clinical strategy of diagnosing and following patients with nonalcoholic fatty liver disease based on invasive and noninvasive methods. J Gastroenterol. 2018;53:181–96.
13. Tang A, Cloutier G, Szeverenyi NM, et al. Ultrasound elastography and MR elastography for assessing liver fibrosis: part 2, diagnostic performance, confounders, and future directions. AJR Am J Roentgenol. 2015;205:33–40.
14. Muthupillai R, Lomas DJ, Rossman PJ, et al. Magnetic resonance elastography by direct visualization of propagating acoustic strain waves. Science. 1995;269:1854–7.
15. Venkatesh SK, Yin M, Ehman RL. Magnetic resonance elastography of liver: technique, analysis, and clinical applications. J Magn Reson Imaging. 2013;37:544–55.
16. Barr RG, Ferraioli G, Palmeri ML, et al. Elastography assessment of liver fibrosis: society of radiologists in ultrasound consensus conference statement. Radiology. 2015;276:845–61.
17. Srinivasa Babu A, Wells ML, Teytelboym OM, et al. Elastography in chronic liver disease: modalities, techniques, limitations, and future directions. RadioGraphics. 2016;36:1987–2006.
18. Venkatesh SK, Talwalkar JA. When and how to use magnetic resonance elastography for patients with liver disease in clinical practice. Am J Gastroenterol. 2018;113:923–6.
19. Carrión JA, Navasa M, Forns X. MR elastography to assess liver fibrosis. Radiology. 2008;247:591 ((**author reply 591–2**)).
20. Barr RG. Elastography in clinical practice. Radiol Clin North Am. 2014;52:1145–62.
21. Tan CH, Venkatesh SK. Magnetic resonance elastography and other magnetic resonance imaging techniques in chronic liver disease: current status and future directions. Gut Liver. 2016;10:672–86.
22. Loomba R, Cui J, Wolfson T, et al. Novel 3D magnetic resonance elastography for the noninvasive diagnosis of advanced

fibrosis in NAFLD: a prospective study. Am J Gastroenterol. 2016;111:986–94.
23. Yin M, Talwalkar JA, Glaser KJ, et al. Assessment of hepatic fibrosis with magnetic resonance elastography. Clin Gastroenterol Hepatol. 2007;5:e2.
24. Hines CD, Bley TA, Lindstrom MJ, et al. Repeatability of magnetic resonance elastography for quantification of hepatic stiffness. J Magn Reson Imaging. 2010;31:725–31.
25. Shire NJ, Yin M, Chen J, et al. Test-retest repeatability of MR elastography for noninvasive liver fibrosis assessment in hepatitis C. J Magn Reson Imaging. 2011;34:947–55.
26. Trout AT, Serai S, Mahley AD, et al. Liver stiffness measurements with MR elastography: agreement and repeatability across imaging systems, field strengths, and pulse sequences. Radiology. 2016;281:793–804.
27. Yasar TK, Wagner M, Bane O, et al. Interplatform reproducibility of liver and spleen stiffness measured with MR elastography. J Magn Reson Imaging. 2016;43:1064–72.
28. Gill HE, Lisanti CJ, Schwope RB, et al. Technical success rate of MR elastography in a population without known liver disease. Abdom Radiol (NY). 2020. https://doi.org/10.1007/s00261-020-02652-x.
29. Singh S, Venkatesh SK, Loomba R, et al. Diagnostic performance of magnetic resonance elastography in staging liver fibrosis: a systematic review and meta-analysis of individual participant data. Clin Gastroenterol Hepatol. 2015;13:e6.
30. Yin M, Talwalkar JA, Glaser KJ, et al. Dynamic postprandial hepatic stiffness augmentation assessed with MR elastography in patients with chronic liver disease. AJR Am J Roentgenol. 2011;197:64–70.
31. Kim D, Kim WR, Talwalkar JA, et al. Advanced fibrosis in nonalcoholic fatty liver disease: noninvasive assessment with MR elastography. Radiology. 2013;268:411–9.
32. Loomba R, Wolfson T, Ang B, et al. Magnetic resonance elastography predicts advanced fibrosis in patients with nonalcoholic fatty liver disease: a prospective study. Hepatology. 2014;60:1920–8.
33. Singh S, Venkatesh SK, Loomba R, et al. Magnetic resonance elastography for staging liver fibrosis in non-alcoholic fatty liver disease: a diagnostic accuracy systematic review and individual participant data pooled analysis. Eur Radiol. 2016;26:1431–40.
34. Imajo K, Kessoku T, Honda Y, et al. Magnetic resonance imaging more accurately classifies steatosis and fibrosis in patients with nonalcoholic fatty liver disease than transient elastography. Gastroenterology. 2016;150:e7.
35. Cui J, Heba E, Hernandez C, et al. Magnetic resonance elastography is superior to acoustic radiation force impulse for the diagnosis of fibrosis in patients with biopsy-proven nonalcoholic fatty liver disease: a prospective study. Hepatology. 2016;63:453–61.
36. Park CC, Nguyen P, Hernandez C, et al. Magnetic resonance elastography vs transient elastography in detection of fibrosis and noninvasive measurement of steatosis in patients with biopsy-proven nonalcoholic fatty liver disease. Gastroenterology. 2017;152:e2.
37. Schwimmer JB, Behling C, Angeles JE, et al. Magnetic resonance elastography measured shear stiffness as a biomarker of fibrosis in pediatric nonalcoholic fatty liver disease. Hepatology. 2017;66:1474–85.
38. Hsu C, Caussy C, Imajo K, et al. Magnetic resonance vs transient elastography analysis of patients with nonalcoholic fatty liver disease: a systematic review and pooled analysis of individual participants. Clin Gastroenterol Hepatol. 2019;17:e8.
39. Xiao G, Zhu S, Xiao X, et al. Comparison of laboratory tests, ultrasound, or magnetic resonance elastography to detect fibrosis in patients with nonalcoholic fatty liver disease: a meta-analysis. Hepatology. 2017;66:1486–501.
40. Dulai PS, Sirlin CB, Loomba R. MRI and MRE for non-invasive quantitative assessment of hepatic steatosis and fibrosis in NAFLD and NASH: clinical trials to clinical practice. J Hepatol. 2016;65:1006–16.
41. Ajmera VH, Liu A, Singh S, et al. Clinical utility of an increase in magnetic resonance elastography in predicting fibrosis progression in nonalcoholic fatty liver disease. Hepatology. 2020;71:849–60.
42. Honda Y, Yoneda M, Imajo K, et al. Elastography techniques for the assessment of liver fibrosis in non-alcoholic fatty liver disease. Int J Mol Sci. 2020;21:4039.
43. Lee SS, Park SH. Radiologic evaluation of nonalcoholic fatty liver disease. World J Gastroenterol. 2014;20:7392–402.
44. Grimm A, Meyer H, Nicke MD, et al. Evaluation of 2-point, 3-point, and 6-point Dixon magnetic resonance imaging with flexible echo timing for muscle fat quantification. Eur J Radiol. 2018;103:57–64.
45. Negrete LM, Middleton MS, Clark L, et al. Inter-examination precision of magnitude-based MRI for estimation of segmental hepatic proton density fat fraction in obese subjects. J Magn Reson Imaging. 2014;39:1265–71.
46. Tyagi A, Yeganeh O, Levin Y, et al. Intra- and inter-examination repeatability of magnetic resonance spectroscopy, magnitude-based MRI, and complex-based MRI for estimation of hepatic proton density fat fraction in overweight and obese children and adults. Abdom Imaging. 2015;40:3070–7.
47. Bannas P, Kramer H, Hernando D, et al. Quantitative magnetic resonance imaging of hepatic steatosis: validation in ex vivo human livers. Hepatology. 2015;62:1444–55.
48. Vu KN, Gilbert G, Chalut M, et al. MRI-determined liver proton density fat fraction, with MRS validation: comparison of regions of interest sampling methods in patients with type 2 diabetes. J Magn Reson Imaging. 2016;43:1090–9.
49. Permutt Z, Le TA, Peterson MR, et al. Correlation between liver histology and novel magnetic resonance imaging in adult patients with non-alcoholic fatty liver disease: MRI accurately quantifies hepatic steatosis in NAFLD. Aliment Pharmacol Ther. 2012;36:22–9.
50. Tang A, Tan J, Sun M, et al. Nonalcoholic fatty liver disease: MR imaging of liver proton density fat fraction to assess hepatic steatosis. Radiology. 2013;267:422–31.
51. Di Martino M, Pacifico L, Bezzi M, et al. Comparison of magnetic resonance spectroscopy, proton density fat fraction and histological analysis in the quantification of liver steatosis in children and adolescents. World J Gastroenterol. 2016;22:8812–9.
52. Rung JH, Smits LP, Verheij J, et al. MR spectroscopy-derived proton density fat fraction is superior to controlled attenuation parameter for detecting and grading hepatic steatosis. Radiology. 2018;286:547–56.
53. Chen J, Talwalkar JA, Yin M, et al. Early detection of nonalcoholic steatohepatitis in patients with nonalcoholic fatty liver disease by using MR elastography. Radiology. 2011;259:749–56.
54. Singh S, Allen AM, Wang Z, et al. Fibrosis progression in nonalcoholic fatty liver vs. nonalcoholic steatohepatitis: a systematic review and meta-analysis of paired-biopsy studies. Clin Gastroenterol Hepatol. 2015;13:e1.
55. Castera L, Friedrich-Rust M, Loomba R. Noninvasive assessment of liver disease in patients with nonalcoholic fatty liver disease. Gastroenterology. 2019;156:e4.
56. Harrison SA, Dennis A, Fiore MM, et al. Utility and variability of three non-invasive liver fibrosis imaging modalities to evaluate efficacy of GR-MD-02 in subjects with NASH and bridging fibrosis during a phase-2 randomized clinical trial. PLoS ONE. 2018;13:e0203054.
57. Chen J, Yin M, Talwalkar JA, et al. Diagnostic performance of MR elastography and vibration-controlled transient elastography

in the detection of hepatic fibrosis in patients with severe to morbid obesity. Radiology. 2017;283:418–28.
58. Wagner M, Corcuera-Solano I, Lo G, et al. Technical failure of MR elastography examinations of the liver: experience from a large single-center study. Radiology. 2017;284:401–12.
59. Harrison SA, Bashir MR, Guy CD, et al. Resmetirom (MGL-3196) for the treatment of non-alcoholic steatohepatitis: a multicentre, randomised, double-blind, placebo-controlled, phase 2 trial. Lancet. 2019;394:2012–24.
60. Caussy C, Reeder SB, Sirlin CB, et al. Noninvasive, quantitative assessment of liver fat by MRI-PDFF as an endpoint in NASH Trials. Hepatology. 2018;68:763–72.
61. Dennis A, Mouchti S, Kelly M, Fallowfield JA, Hirschfield G, Pavlides M, Banerjee R. A composite biomarker using multiparametric magnetic resonance imaging and blood analytes accurately identifies patients with non-alcoholic steatohepatitis and significant fibrosis. Sci Rep. 2020;10(1):15308. https://doi.org/10.1038/s41598-020-71995-8.
62. Jayakumar S, Middleton MS, Lawitz EJ, et al. Longitudinal correlations between MRE, MRI-PDFF, and liver histology in patients with non-alcoholic steatohepatitis: analysis of data from a phase II trial of selonsertib. J Hepatol. 2019;70:133–41.
63. Eddowes PJP, McDonald N, Davies N, et al. Utility and cost evaluation of multiparametric magnetic resonance imaging for the assessment of non-alcoholic fatty liver disease. Aliment Pharmacol Ther. 2018;47:631–44.
64. Pavlides M, Banerjee R, Sellwood J, et al. Multiparametric magnetic resonance imaging predicts clinical outcomes in patients with chronic liver disease. J Hepatol. 2016;64:308–15.
65. Bachtiar V, Kelly MD, Wilman HR, et al. Repeatability and reproducibility of multiparametric magnetic resonance imaging of the liver. PLoS ONE. 2019;14:e0214921.
66. Abrigo JM, Shen J, Wong VW, et al. Non–alcoholic fatty liver disease: spectral patterns observed from an in vivo phosphorus magnetic resonance spectroscopy study. J Hepatol. 2014;60:809–15.
67. Kim T, Jun HY, Kim K, et al. Hepatic alanine differentiates nonalcoholic steatohepatitis from simple steatosis in humans and mice: a proton MR spectroscopy study with long echo time. J Magn Reson Imaging. 2017;46:1298–310.
68. Leporq B, Lambert SA, Ronot M, et al. Simultaneous MR quantification of hepatic fat content, fatty acid composition, transverse relaxation time and magnetic susceptibility for the diagnosis of non-alcoholic steatohepatitis. NMR Biomed. 2017. https://doi.org/10.1002/nbm.3766.
69. Parente DB, Paiva FF, Neto JA, et al. Intravoxel incoherent motion diffusion weighted MR imaging at 3.0 T: assessment of steatohepatitis and fibrosis compared with liver biopsy in type 2 diabetic patients. PLoS ONE. 2015;10:e0125653.
70. Dillman JR, Trout AT, Costello EN, et al. Quantitative liver MRI biopsy correlation in pediatric and young adult patients with nonalchohlic fatty liver disease: can one be used to predict the other? AJR Am J Roentgenol. 2018;210:166–74.
71. Parente D, Oliveira Neto J, Brasil P, et al. Preperitoneal fat as a non-invasive marker of increased risk of severe non–alcoholic fatty liver disease in patients with type 2 diabetes. J Gastroenterol Hepatol. 2018;33:511–7.
72. Gallego-Durán R, Cerro-Salido P, Gomez-Gonzalez E, et al. Imaging biomarkers for steatohepatitis and fibrosis detection in non-alcoholic fatty liver disease. Sci Rep. 2016;6:31421.
73. Bastati N, Feier D, Wibmer A, et al. Noninvasive differentiation of simple steatosis and steatohepatitis by using gadoxetic acid–enhanced MR imaging in patients with disease: a proof-of-concept study. Radiology. 2014;271:739–47.
74. Smits L, Coolen B, Panno M, et al. Noninvasive differentiation between hepatic steatosis and steatohepatitis with MR imaging enhanced with USPIOs in patients with nonalcoholic fatty liver disease: a proof-of-concept study. Radiology. 2016;278:782–91.
75. Tomita K, Tanimoto A, Irie R, et al. Evaluating the severity of nonalcoholic steatohepatitis with superparamagnetic iron oxide-enhanced magnetic resonance imaging. J Magn Reson Imaging. 2008;28:1444–50.
76. Klatt D, Hamhaber U, Asbach P, et al. Noninvasive assessment of the rheological behavior of human organs using multifrequency MR elastography: a study of brain and liver viscoelasticity. Phys Med Biol. 2007;52:7281–94.
77. Asbach P, Klatt D, Hamhaber U, et al. Assessment of liver viscoelasticity using multifrequency MR elastography. Magn Reson Med. 2008;60:373–9.
78. Meyer GA, McCulloch AD, Lieber RL. A nonlinear model of passive muscle viscosity. J Biomech Eng. 2011;133(9):091007. https://doi.org/10.1115/1.4004993.
79. Sack I, Beierbach B, Wuerfel J, et al. The impact of aging and gender on brain viscoelasticity. Neuroimage. 2009;46:652–7.
80. Wuerfel J, Paul F, Beierbach B, et al. MR-elastography reveals degradation of tissue integrity in multiple sclerosis. Neuroimage. 2010;49:2520–5.
81. de Franchis R, Baveno VI Faculty. Expanding consensus in portal hypertension: report of the Baveno VI consensus workshop: stratifying risk and individualizing care for portal hypertension. J Hepatol. 2014;63:743–52.
82. Ronot M, Lambert S, Elkrief L, et al. Assessment of portal hypertension and high-risk oesophageal varices with liver and spleen three-dimensional multifrequency MR elastography in liver cirrhosis. Eur Radiol. 2014;24:1394–402.
83. Sun HY, Lee JM, Han JK, Choi BI. Usefulness of MR elastography for predicting esophageal varices in cirrhotic patients. J Magn Reson Imaging. 2014;39:559–66.
84. Matsui N, Imajo K, Yoneda M, et al. Magnetic resonance elastography increases usefulness and safety of non-invasive screening for esophageal varices. J Gastroenterol Hepatol. 2018;33:2022–8.
85. Ma X, Wang L, Wu H, et al. Spleen stiffness is superior to liver stiffness for predicting esophageal varices in chronic liver disease: a meta-analysis. PLoS ONE. 2016;11:1–15.
86. Levick C, Phillips-Hughes J, Collier J, et al. Non-invasive assessment of portal hypertension by multi-parametric magnetic resonance imaging of the spleen: a proof of concept study. PLoS ONE. 2019;14:e0221066.
87. Nedredal GI, Yin M, McKenzie T, et al. Portal hypertension correlates with splenic stiffness as measured with MR elastography. J Magn Reson Imaging. 2011;34:79–87.
88. Shin SU, Lee JM, Yu MH, et al. Prediction of esophageal varices in patients with cirrhosis: usefulness of three-dimensional MR elastography with echo-planar imaging technique. Radiology. 2014;272:143–53.
89. Yin M, Glaser KJ, Talwalkar JA, et al. Hepatic MR elastography: clinical performance in a series of 1377 consecutive examinations. Radiology. 2016;278:114–24.
90. Millonig G, Reimann FM, Friedrich S, et al. Extrahepatic cholestasis increases liver stiffness (FibroScan) irrespective of fibrosis. Hepatology. 2008;48:1718–23.
91. Coco B, Oliveri F, Maina AM, et al. Transient elastography: a new surrogate marker of liver fibrosis influenced by major changes of transaminases. J Viral Hepat. 2007;14:360–9.
92. European Association for the Study of the Liver (EASL); European Association for the Study of Diabetes (EASD); European Association for the Study of Obesity (EASO). EASL-EASD-EASO Clinical Practice Guidelines for the management of non-alcoholic fatty liver disease. J Hepatol. 2016;64:1388–402.
93. Sasso M, Beaugrand M, de Ledinghen V, et al. Controlled attenuation parameter (CAP): a novel VCTE™ guided ultrasonic attenuation measurement for the evaluation of hepatic steatosis:

preliminary study and validation in a cohort of patients with chronic liver disease from various causes. Ultrasound Med Biol. 2010;36:1825–35.
94. Newsome PN, Sasso M, Deeks JJ, et al. FibroScan-AST (FAST) score for the non-invasive identification of patients with non-alcoholic steatohepatitis with significant activity and fibrosis: a prospective derivation and global validation study. Lancet Gastroenterol Hepatol. 2020;5:362–73.
95. Oeda S, Takahashi H, Imajo K, et al. Diagnostic accuracy of FibroScan-AST score to identify non-alcoholic steatohepatitis with significant activity and fibrosis in Japanese patients with non-alcoholic fatty liver disease: comparison between M and XL probes. Hepatol Res. 2020;50:831–9.
96. Reeder SB, Robson PM, Yu H, et al. Quantification of hepatic steatosis with MRI: the effects of accurate fat spectral modeling. J Magn Reson Imaging. 2009;29:1332–9.
97. Yoneda M, Imajo K, Nakajima A. Non-invasive diagnosis of nonalcoholic fatty liver disease. Am J Gastroenterol. 2018;113:1409–11.
98. Chan WK, Treeprasertsuk S, Goh GB, et al. Optimizing use of nonalcoholic fatty liver disease fibrosis score, Fibrosis-4 Score, and liver stiffness measurement to identify patients with advanced fibrosis. Clin Gastroenterol Hepatol. 2019;17:e37.